AIAA SciTech
5-9 January 2015, Kissimmee, Florida
AIAA Infotech @ Aerospace

# Unmanned Aircraft System Sense and Avoid Integrity and Continuity Risk for Non-Cooperatve Intruders

Michael B. Jamoom,* Mathieu Joerger† and Boris Pervan‡
*Illinois Institute of Technology, Chicago, IL, 60616, USA*

**This paper describes new methods to quantify safety of sense and avoid (SAA) functions for Unmanned Aircraft Systems (UAS) by evaluating integrity and continuity risks. These methods can set sensor requirements. The closest point of approach (CPA) distance and time to CPA, tau, are used to measure the hazards associated with the intruder aircraft. This paper presents a method to determine hazard state estimates and estimate error. These variances are used to establish (1) the integrity risk of the SAA system not detecting imminent loss of self-separation and (2) the probability of false alert, the continuity risk. A preliminary analysis assumes a constant relative velocity model with normal, independent and stationary measurement errors. A sensitivity analysis evaluates the impact on integrity and continuity of sensor noise, range and sample interval. This research can set potential SAA sensor requirements for UAS integration into the National Airspace System.**



## Nomenclature

| | |
|---|---|
| $\tau$ | Time to Closest Point of Approach (CPA), seconds |
| $r_{CPA}$ | Horizontal Distance from Own-Aircraft to CPA, feet |
| $z_{CPA}$ | Vertical Distance from Own-Aircraft to CPA, feet |
| $P_{HMI}$ | Probability of Hazardously Misleading Information (HMI) |
| $P_{FA}$ | Probability of False Alert (FA) |
| $\tau_{SS}$ | $\tau$ self-separation threshold, seconds |
| $r_{MD}$ | Horizontal Miss Distance (MD) CPA threshold, feet |
| $z_{MD}$ | Vertical MD CPA threshold, feet |
| $x, y, z$ | Cartesian Intruder Position, feet |
| $\mathbf{x}_0$ | Initial Intruder Position Vector, feet |
| $r$ | Intruder Horizontal Range, feet |
| $\rho$ | Intruder Slant Range, feet |
| $\theta$ | Intruder Azimuth Angle |
| $\phi$ | Intruder Elevation Angle |
| $t_n$ | Time at Sample $n$, seconds |
| $\Delta t$ | Sample Interval, seconds |
| $n$ | Sample Number |
| $\mathbf{z}$ | Intruder Measurement Vector, feet |
| $\mathbf{v}$ | Measurement Error Vector, feet |
| $\mathbf{V}$ | Measurement Error Covariance Matrix, square feet |
| $\sigma$ | Standard Deviation |
| $\dot{\mathbf{x}}$ | Intruder Constant Velocity Vector, feet/second |
| $\mathbf{x}$ | Trajectory State Vector: Initial Position and Constant Velocity $[\ \mathbf{x}_0 \quad \dot{\mathbf{x}}\ ]^T$ |

*PhD Candidate, Department of Mechanical, Materials and Aerospace Engineering, 10 W 32nd Street, Room 243, Student Member AIAA.
†Research Assistant Professor, Department of Mechanical, Materials and Aerospace Engineering, 10 W 32nd Street, Room 243, Senior Member AIAA.
‡Professor, Department of Mechanical, Materials and Aerospace Engineering, 10 W 32nd Street, Room 243, Associate Fellow AIAA.

| | |
|---|---|
| $\mathbf{H}$ | Observation Matrix |
| $\hat{\mathbf{x}}$ | Trajectory State Estimate Vector, feet |
| $\hat{\mathbf{P}}$ | Trajectory State Estimate Error Covariance Matrix, square feet |
| $\mathbf{x}_{CPA}$ | CPA Distance Vector, feet |
| $\mathbf{a}$ | Hazard State Transformation Vector |
| $\hat{\tau}$ | Estimated Time to CPA, seconds |
| $\hat{r}_{CPA}$ | Estimated Horizontal CPA Distance, feet |
| $\hat{z}_{CPA}$ | Estimated Vertical CPA Distance, feet |
| $\mathbf{P}_{\tau rz}$ | Full Hazard State Covariance Matrix |
| $\mathbf{A}$ | Full Hazard State Transformation Matrix |
| $k$ | Integrity Coefficient |
| $\ell$ | Continuity Coefficient |
| $Q(x)$ | Tail Probability Function for Standard Normal Distribution |
| $\Phi(x)$ | Cumulative Distribution Function for Standard Normal Distribution |
| $I_{SS}$ | Integrity Requirement for Self-Separation |
| $C_{SS}$ | Continuity Requirement for Self-Separation |
| $\mu$ | Very Small Value |
| $\epsilon$ | Operational Limit Percentage |
| $\tilde{\sigma}$ | Standard Deviation Operational Limit |
| $\tilde{\tau}$ | Time to CPA Operational Limit, seconds |
| $\tilde{r}$ | Intruder Horizontal Range Operational Limit, feet |
| $\tilde{z}$ | Intruder Vertical Range Operational Limit, feet |
| *Subscript* | |
| $n$ | Sample Number |
| $N$ | Designates variables at Samples 0 to $n$: $N = 0, \ldots, n$ |
| $x, y, z$ | Relating to Cartesian Intruder Position |
| $r$ | Relating to Intruder Horizontal Range |
| $\tau$ | Relating to time to CPA |
| $\rho, \theta, \phi$ | Relating to Spherical Intruder Position |



# I. Introduction

## I.A. The Need for Sense and Avoid

For the last two decades, unmanned aircraft systems (UAS) have operated on a limited basis in the National Airspace System (NAS) supporting mostly public functions like military operations and border security.[1] UAS operations are rapidly expanding to encompass a wider range of civil and commercial applications, including photography, agriculture and communications.[1] With increased interest in UAS, the United States Congress mandated the Federal Aviation Administration (FAA), through the *FAA Modernization and Reform Act of 2012*, to develop requirements necessary for broader UAS access into the NAS.[2] One of the challenges the FAA faces in meeting this mandate is ensuring an acceptable level of safety. To ensure safety, a UAS requires a "sense and avoid" (SAA) capability to provide self-separation and collision avoidance (CA) protection between the UAS and other aircraft analogous to the "see and avoid" responsibility for pilots of manned aircraft.[1]

Depending of the class of controlled airspace, if an intruder aircraft is cooperative, that is, employing an operating transponder or Automatic Dependent Surveillance - Broadcast (ADS-B),[3] air traffic control (ATC) may provide separation. Alternatively, a manned aircraft pilot could employ a Traffic Collision Avoidance System (TCAS) as a situational awareness aid to help the pilot detect the intruder then initiate an avoidance maneuver. Otherwise, if the intruder aircraft is non-cooperative, without an operating transponder or ADS-B, the manned aircraft pilot will not have the help of ATC or TCAS. In this manned aircraft case, it is solely the pilot's responsibility to visually see the intruder and maneuver to maintain separation. Since UAS will not have a pilot on board, it will have to replicate the functionality of pilot vision through an appropriate sensor. Detection of non-cooperative aircraft will require, for example, an electro-optical (EO), infrared (IR) or radar sensor. This sensor must adequately inform the UAS SAA system whether or not a separation

maneuver is required.

### I.B. Self-Separation and Collision Avoidance

The Second FAA-Sponsored SAA Workshop Caucus concluded that although self-separation is a widely recognized term by the FAA and International Civil Aviation Organization (ICAO), it has never been fully codified.[4] They also concluded that the well clear threshold (WCT) is a separation standard that could be used for developing UAS SAA system self-separation functionality.[4] "Well clear" is a term subjectively referenced in the US Code of Federal Regulations (CFR) 14 CFR 91.113 in reference to right-of-way rules.[5] Weibel's paper,[6] makes a case to use well clear as a separation standard. In August 2014, the RTCA Special Committee-228 (SC-228) defined well clear as having a time to closest point of approach (CPA), $\tau$, of 35 seconds, a horizontal miss distance of 4000 feet and a vertical miss distance of 700 feet.[7]

When an intruder cannot remain well clear, a CA maneuver is required to avoid a near mid-air collision (NMAC). NMAC boundaries are typically 500 feet laterally and 100 feet vertically from the own aircraft.[4] If the intruder aircraft is non-cooperative, it is up to the UAS SAA system to provide the appropriate CA maneuver.

Figure 1 depicts the conceptual difference between the WCT and NMAC distance thresholds (not to scale). For simplicity, this paper will concentrate on self-separation and WCT. The methodology is the same for collision avoidance and NMAC.

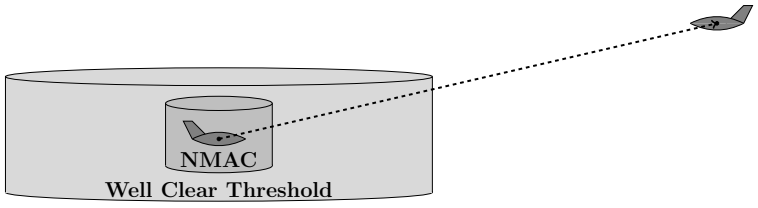


**Figure 1. Well Clear Threshold and Near Mid-Air Collision**

### I.C. Problem Statement and Response

SAA safety performance needs to be quantified as a function of sensor uncertainty, and if possible, using high-level requirements that apply to a wide variety of sensors. In response, in this paper, we define *integrity risk* and *continuity risk* as UAS SAA safety performance metrics. This paper provides methods to evaluate integrity and continuity risk that can also be used to establish sensor performance requirements. These requirements will ensure a predefined level of safety. This paper also maps and bounds the trade space of requirements necessary to maintain desired integrity and continuity.

### I.D. Integrity Risk

Integrity risk is the probability that the system provides Hazardously Misleading Information (HMI), which is an unacceptably large error without a timely warning that the system cannot be trusted.[8] For the SAA problem, HMI occurs when the SAA system is not sensing a hazard (and not alerting to maneuver) but in fact, a hazard is present and a self-separation maneuver is required.

The Second SAA Workshop Caucus concluded that the hazard severity classification is always "catastrophic" for CA and always "major" for failing to maintain well clear.[4] According to FAA Advisory Circular (AC) 25.1309-1A, catastrophic failure conditions must be "extremely improbable" and major failure conditions must be "improbable."[9] It goes on to define extremely improbable failure conditions as having probability on the order of $10^{-9}$ or less and improbable failure conditions as having probability between $10^{-5}$ and $10^{-9}$.[9] Based on those definitions, SAA integrity risk requirements can be selected for self-separation and CA. The self-separation integrity risk should be between $10^{-5}$ and $10^{-9}$ and the CA integrity risk should be $10^{-9}$ or less.

### I.E. Continuity Risk

Continuity is a way to quantify false alert (FA) probability of the SAA system, which is the probability that an integrity monitor issues an alert when no fault is present.[8] When FA's occur, the potential exists for the

UAS to maneuver unexpectedly, resulting in, at best, increased workloads for ATC and pilots of potential intruders or, at worst, an induced self-separation or CA hazard with a different intruder. For the purposes of this research, loss of continuity will be classified as a major hazard, and should be between $10^{-5}$ and $10^{-9}$. This mirrors the continuity breach requirement for GPS-based precision landing of aircraft, which is considered a major hazard.[10]

### I.F. Approach

SAA integrity risk evaluation is presented as a three-dimensional, two-body problem. The two bodies are the own aircraft and the intruder aircraft. The coordinate frame will always be an own-aircraft-centered body frame. For the purposes of this paper, the intruder aircraft is assumed to have a constant relative velocity. A weighted least squares estimator is employed to determine the aircraft relative position and velocity, referred to as the trajectory state estimates, as well as the corresponding trajectory state estimate error covariance.

The hazard states of an intruder that describe an imminent threat are time to CPA, or "tau" ($\tau$), and position of CPA, broken into horizontal distance to CPA, $r_{CPA}$, and vertical distance to CPA, $z_{CPA}$. The WCT self-separation criteria are based on thresholds on $\tau$, $r_{CPA}$, and $z_{CPA}$. The SAA system needs to initiate a self-separation maneuver early enough to ensure the intruder aircraft remains outside the WCT. The tau self-separation threshold, $\tau_{SS}$, represents the minimum time required to initiate the self-separation to prevent a WCT violation. Spatially, the CPA must be within both the WCT horizontal and vertical miss distance (MD), $r_{MD}$ and $z_{MD}$, to be considered a hazard.

Expressions for probability of HMI, $P_{HMI}$, and probability of FA, $P_{FA}$, are presented, and the WCT is adjusted to ensure integrity and continuity. A computationally efficient approach is established to determine bounds on the integrity risk and continuity risk. A sensitivity analysis identifies trade-offs between sensor requirements, sample rates, integrity and continuity. It is then shown how the methods derived can be used to set potential SAA sensor requirements necessary for UAS-NAS integration.

### I.G. Paper Outline

After this introductory section, Section II will frame the SAA problem and provide a methodology for determining the estimates and estimation error covariances of the intruder trajectory states. Next, Section III will define the self-separation hazard parameters and provide a methodology for determining their estimate error variances. Then Section IV outlines the methodology for determining and applying integrity risk. Section V outlines the methodology for determining and applying continuity risk. Section VI relates integrity and continuity to sensor requirements. Section VII includes a sensitivity analysis depicting an example two dimensional measurement model to examine trade-offs between integrity and continuity risk, sensor uncertainty and sample rates. Finally, Section VIII provides conclusions and opportunities for future research.

## II. Relative Intruder State Estimation

We present the SAA problem as a three dimensional, two-body problem. The two bodies are the own aircraft and the intruder aircraft. The coordinate frame will always be an own-aircraft-centered body frame. For the purposes of this problem, the intruder aircraft is assumed to have a constant relative velocity. This is a preliminary analysis and other cases will be addressed in future work.

In the own-aircraft-centered body frame, the relative position of the intruder can be described in spherical, Cartesian or cylindrical coordinates. Figure 2 is a graphical depiction of the own aircraft and the intruder aircraft in the horizontal and vertical planes. In the horizontal plane, we orient the $x$ and $y$ axes such that the $x$-axis is directly out of the nose of the own aircraft. The azimuth, $\theta$ is the angle counterclockwise from the $x$-axis to the horizontal range vector (from the origin to the intruder position on the $xy$-plane). In the vertical plane, $\phi$ is the angle from the $xy$-plane up to the slant range vector (from the origin to the intruder position on the $xz$-plane).

### II.A. Measurement Model

The own aircraft makes a scan at time $t_n$ measuring the the intruder position:

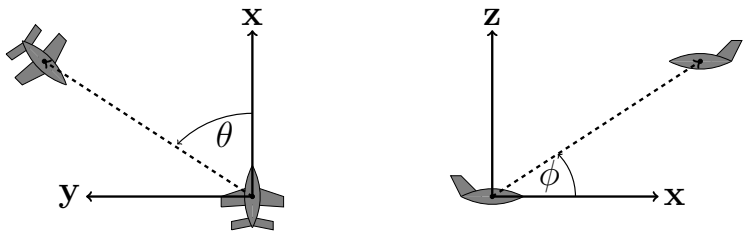


**Figure 2. Horizontal and Vertical Position of the Intruder Aircraft**

$$\mathbf{z}_n = \mathbf{x}_n + \mathbf{v}_n \qquad \mathbf{v}_n \sim N(\mathbf{0}, \mathbf{V}_n) \tag{1}$$

$\mathbf{z}_n$ is the measurement at time $t_n$. $\mathbf{x}_n$ is the intruder position at time $t_n$:

$$\mathbf{x}_n = \begin{bmatrix} x_n & y_n & z_n \end{bmatrix}^T \tag{2}$$

$\mathbf{v}_n$ is the $t_n$ measurement error, which we assume is over-bounded in the cumulative distribution function (CDF) sense by Gaussian distributions.[11,12] The measurement error covariance matrix at each time is $\mathbf{V}_n$. $N(a, b)$ represents a normal distribution with mean $a$ and covariance $b$. We also assume that the sample interval, $\Delta t$, is selected large enough to ensure independence of sequential sensor measurement errors.

### II.B. Constant Velocity Model

We assume constant intruder relative velocity, $\dot{\mathbf{x}}$, over the sample interval $\Delta t$. In this case, $\Delta t$ is between time $t_0$ and time $t_1$ such that $\mathbf{x}_1 = \mathbf{x}_0 + \Delta t \dot{\mathbf{x}}$:

$$\mathbf{z}_1 = \mathbf{x}_0 + \Delta t \dot{\mathbf{x}} + \mathbf{v}_1 \qquad \mathbf{v}_1 \sim N(\mathbf{0}, \mathbf{V}_n) \tag{3}$$

Now we assume a constant velocity over the full measurement time interval, $n\Delta t$. Stacking the measurements in the standard $z = Hx + v$ measurement equation form:

$$\mathbf{z}_N = \mathbf{H}_N \mathbf{x} + \mathbf{v}_N \tag{4}$$

where the full measurement vector, $\mathbf{z}_N$, the full observation matrix, $\mathbf{H}_N$, the trajectory state vector, $\mathbf{x}$, and full measurement error vector, $\mathbf{v}_N$, are:

$$\mathbf{z}_N = \begin{bmatrix} \mathbf{z}_0 & \mathbf{z}_1 & \dots & \mathbf{z}_n \end{bmatrix}^T \tag{5}$$

$$\mathbf{H}_N = \begin{bmatrix} \mathbf{I}_{3x3} & \mathbf{0}_{3x3} \\ \mathbf{I}_{3x3} & \Delta t \mathbf{I}_{3x3} \\ \vdots & \vdots \\ \mathbf{I}_{3x3} & n\Delta t \mathbf{I}_{3x3} \end{bmatrix} \tag{6}$$

$$\mathbf{x} = \begin{bmatrix} \mathbf{x}_0 \\ \dot{\mathbf{x}} \end{bmatrix} = \begin{bmatrix} x_0 & y_0 & z_0 & \dot{x} & \dot{y} & \dot{z} \end{bmatrix}^T \tag{7}$$

$$\mathbf{v}_N = \begin{bmatrix} \mathbf{v}_0 & \mathbf{v}_1 & \dots & \mathbf{v}_n \end{bmatrix}^T \sim N(\mathbf{0}, \mathbf{V}_N) \tag{8}$$

The full measurement error covariance, $\mathbf{V}_N$, for all time steps is a block diagonal matrix of the individual time step measurement error covariance matrices, $\mathbf{V}_n$, which are not necessarily diagonal themselves:

$$\mathbf{V}_N = \begin{bmatrix} \mathbf{V}_0 & \mathbf{0} & \cdots & \mathbf{0} \\ \mathbf{0} & \mathbf{V}_1 & \cdots & \mathbf{0} \\ \vdots & \vdots & \ddots & \vdots \\ \mathbf{0} & \mathbf{0} & \cdots & \mathbf{V}_n \end{bmatrix} \tag{9}$$

To get the trajectory state estimate vector, $\hat{\mathbf{x}}_n$, we use a weighted least squares estimator:

$$\hat{\mathbf{x}}_n = (\mathbf{H}_N^T \mathbf{V}_N^{-1} \mathbf{H}_N)^{-1} \mathbf{H}_N^T \mathbf{V}_N^{-1} \mathbf{z}_N \tag{10}$$

In addition, the corresponding trajectory state estimate error covariance, $\hat{\mathbf{P}}_N$, is then:

$$\hat{\mathbf{P}}_N = (\mathbf{H}_N^T \mathbf{V}_N^{-1} \mathbf{H}_N)^{-1} \tag{11}$$

## III. Hazard States

There are three variables at the CPA that describe a potential hazard with an intruder aircraft, the time to CPA, $\tau$, horizontal distance from origin to CPA, $r_{CPA}$, and vertical distance from origin to CPA, $z_{CPA}$. Figure 3 is an overhead depiction of the CPA. For a WCT violation, first the intruder must be within the WCT. That means $r_{CPA}$ has to be at or within the required horizontal miss distance (MD), $r_{MD}$, and $z_{CPA}$ has to be at or within the vertical miss distance, $z_{MD}$. Both must be true. If the CPA only violates $z_{MD}$, the intruder could be co-altitude at the CPA, but hundreds of miles away. Conversely, if the CPA only violates $r_{MD}$, the intruder could be directly above or below at the CPA, but off altitude by several thousand feet. The other WCT condition required to cause a hazard is a violation of the $\tau$ self-separation threshold, $\tau_{SS}$. This threshold is the minimum time required to initiate the self-separation to prevent $r_{MD}$ and $z_{MD}$ violations. For a hazard to exist, the CPA has to be at or within both the $r_{MD}$ and $z_{MD}$ as well as $\tau$ being less than or equal to $\tau_{SS}$.

### III.A. Time to CPA, $\tau$

In practice, three different approximations are used to determine $\tau$.[4,13] *Simplified* $\tau$ is the range divided by the range rate.[4] *True* $\tau$ is the actual time to CPA assuming unaccelerated flight by both own aircraft and the intruder.[13] Finally, *modified* $\tau$ is time to CPA determined by incorporating a safety factor to account for potential accelerations.[13] This paper uses true $\tau$.

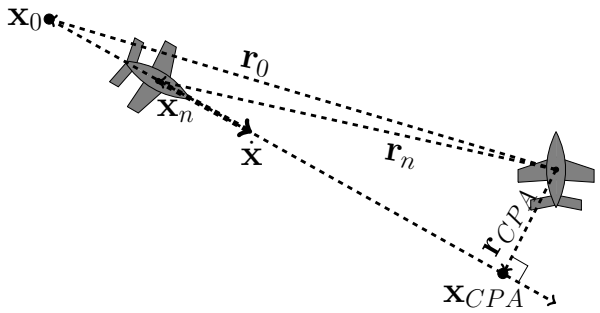


**Figure 3. Overhead View of Closest Point of Approach**

To get true $\tau$ in terms of trajectory states, the following two equations need to be solved:

$$\mathbf{x}_n + \tau \dot{\mathbf{x}} = \mathbf{x}_{CPA} \tag{12}$$

$$\dot{\mathbf{x}} \bullet \mathbf{x}_{CPA} = 0 \tag{13}$$

The first equation reflects the distance from the current position, $\mathbf{x}_n$, to the CPA, $\mathbf{x}_{CPA}$, as a sum of position and $\tau$ times velocity, $\dot{\mathbf{x}}$. The second equation expresses that the velocity vector, $\dot{\mathbf{x}}$, and the vector from the origin to CPA, $\mathbf{x}_{CPA}$, are perpendicular. Combining these equations lead to four equations and four unknowns:

$$\begin{bmatrix} 1 & 0 & 0 & -\dot{x} \\ 0 & 1 & 0 & -\dot{y} \\ 0 & 0 & 1 & -\dot{z} \\ \dot{x} & \dot{y} & \dot{z} & 0 \end{bmatrix} \begin{bmatrix} x_{CPA} \\ y_{CPA} \\ z_{CPA} \\ \tau_n \end{bmatrix} = \begin{bmatrix} x_n \\ y_n \\ z_n \\ 0 \end{bmatrix} \tag{14}$$

The resulting four unknowns, $\tau_n$, $x_{CPA}$, $y_{CPA}$, and $z_{CPA}$ are:

$$\tau_n = \frac{-(\dot{x}x_n + \dot{y}y_n + \dot{z}z_n)}{\dot{x}^2 + \dot{y}^2 + \dot{z}^2} \tag{15}$$

$$\mathbf{x}_{CPA} = \begin{bmatrix} x_{CPA} \\ y_{CPA} \\ z_{CPA} \end{bmatrix} = \begin{bmatrix} x_n + \tau_n\dot{x} \\ y_n + \tau_n\dot{y} \\ z_n + \tau_n\dot{z} \end{bmatrix} \tag{16}$$

To get $\tau$ in terms of the elements of trajectory state vector, $\mathbf{x}$, apply $\mathbf{x}_n = \mathbf{x}_0 + n\Delta t\dot{\mathbf{x}}$:

$$\tau_n = \frac{-(\dot{x}x_0 + \dot{y}y_0 + \dot{z}z_0 + n\Delta t\dot{x}^2 + n\Delta t\dot{y}^2 + n\Delta t\dot{z}^2)}{\dot{x}^2 + \dot{y}^2 + \dot{z}^2} \tag{17}$$

### III.B. Horizontal CPA Position, $r_{CPA}$, and Vertical CPA Position, $z_{CPA}$

Referring to Figure 3, $\mathbf{x}_{CPA}$ is expressed in terms of $\mathbf{x}_n$, $\dot{\mathbf{x}}$, and $\tau_n$:

$$\mathbf{x}_{CPA} = \mathbf{x}_n + \tau_n\dot{\mathbf{x}} \tag{18}$$

$\mathbf{x}_{CPA}$ was found in equation (16). To get the final $\mathbf{x}_{CPA}$ in terms of $\mathbf{x}$, we first apply $\mathbf{x}_n = \mathbf{x}_0 + n\Delta t\dot{\mathbf{x}}$. Then we set $n = 0$ since the CPA distance does not change with time for the constant velocity model:

$$\mathbf{x}_{CPA} = \begin{bmatrix} x_0 + \tau_0\dot{x} \\ y_0 + \tau_0\dot{y} \\ z_0 + \tau_0\dot{z} \end{bmatrix} \tag{19}$$

where $\tau_0$ is the initial $\tau$:

$$\tau_0 = \frac{-(\dot{x}x_0 + \dot{y}y_0 + \dot{z}z_0)}{\dot{x}^2 + \dot{y}^2 + \dot{z}^2} \tag{20}$$

The CPA horizontal range, $r_{CPA}$, is then:

$$r_{CPA} = \sqrt{x_{CPA}^2 + y_{CPA}^2} = \sqrt{(x_0 + \tau_0\dot{x})^2 + (y_0 + \tau_0\dot{y})^2} \tag{21}$$

and $z_{CPA}$ is the $z$ portion of equation (19):

$$z_{CPA} = z_0 + \tau_0\dot{z} \tag{22}$$

### III.C. Hazard State Estimate Error Variance

To get *hazard state* estimate error variances, we first linearize equations (17), (21), and (22). For example, the $\tau$ transformation, $\mathbf{a}_{\tau_n}^T$, is a vector of the Taylor Series partial derivatives of $\tau$ with respect to trajectory states:

$$\mathbf{a}_{\tau_n}^T = \begin{bmatrix} \frac{\partial\tau_n}{\partial x_0}\Big|_{\bar{\mathbf{x}}} & \frac{\partial\tau_n}{\partial y_0}\Big|_{\bar{\mathbf{x}}} & \frac{\partial\tau_n}{\partial z_0}\Big|_{\bar{\mathbf{x}}} & \frac{\partial\tau_n}{\partial \dot{x}}\Big|_{\bar{\mathbf{x}}} & \frac{\partial\tau_n}{\partial \dot{y}}\Big|_{\bar{\mathbf{x}}} & \frac{\partial\tau_n}{\partial \dot{z}}\Big|_{\bar{\mathbf{x}}} \end{bmatrix} \tag{23}$$

where $\bar{\mathbf{x}}$ is an a-priori estimate of the trajectory states. Then, for time $t_n$, we determine the $\tau$ estimate error variance, $\sigma_{\tau_n}^2$, by transforming $\hat{\mathbf{P}}_N$ from equation (11):

$$\sigma_{\tau_n}^2 = \mathbf{a}_{\tau_n}^T\hat{\mathbf{P}}_N\mathbf{a}_{\tau_n} \tag{24}$$

Given zero-mean sensor measurement errors, the resulting distribution for the estimated $\tau$ is:

$$\hat{\tau}_n \sim N(\tau_n, \sigma_{\tau_n}^2) \tag{25}$$

We determine the variance of the CPA distance estimates, $\hat{r}_{CPA}$ and $\hat{z}_{CPA}$, using the same procedure as $\tau$:

$$\sigma_{r_n}^2 = \mathbf{a}_{r_n}^T\hat{\mathbf{P}}_N\mathbf{a}_{r_n} \tag{26}$$

$$\sigma_{z_n}^2 = \mathbf{a}_{z_n}^T\hat{\mathbf{P}}_N\mathbf{a}_{z_n} \tag{27}$$

where $\mathbf{a}_{r_n}^T$ and $\mathbf{a}_{z_n}^T$ are the vectors of Taylor Series partials with respect to each trajectory state for $r_{CPA}$ and $z_{CPA}$. The resulting distributions for the estimated parameters $\hat{r}_{CPA}$ and $\hat{z}_{CPA}$ are:

$$\hat{r}_{CPA} \sim N(r_{CPA}, \sigma_{r_n}^2) \tag{28}$$

$$\hat{z}_{CPA} \sim N(z_{CPA}, \sigma_{z_n}^2) \tag{29}$$

The hazard state estimates ($\hat{\tau}_n$, $\hat{r}_{CPA}$, and $\hat{z}_{CPA}$) are correlated. To get the full covariance matrix, $\mathbf{P}_{\tau r z_n}$, we stack the Taylor Series partial vectors into one matrix, $\mathbf{A}_n$:

$$\mathbf{A}_n = \begin{bmatrix} \mathbf{a}_{\tau_n}^T \\ \mathbf{a}_{r_n}^T \\ \mathbf{a}_{z_n}^T \end{bmatrix} \tag{30}$$

We then apply the measurement covariance matrix, $\hat{\mathbf{P}}_N$, to get $\mathbf{P}_{\tau r z_n}$:

$$\mathbf{P}_{\tau r z_n} = \mathbf{A}_n \hat{\mathbf{P}}_N \mathbf{A}_n^T \tag{31}$$

## IV. Integrity Risk

This section quantifies SAA sensor safety by determining integrity risk based on the three hazard states. As an illustrative example, we first assume the CPA distance will be less than the WCT horizontal and vertical miss distances and base integrity risk solely on $\tau$. Then we remove that assumption and base integrity risk on all three hazard states.

### IV.A. Integrity Risk Based Solely on $\tau$

HMI occurs when a hazard exists, but that hazard is not sensed. Accounting for $\tau$ only, a hazard exists when $\tau \leq \tau_{SS}$. The hazard is not sensed if $\hat{\tau} > \tau_{SS}$. This HMI leads the own aircraft to not maneuver when a self-separation maneuver is warranted.

The left curve in Figure 4 depicts the normal distribution of the estimate, $\hat{\tau}$ (for simplicity, $n$ subscripts are dropped for the rest of the paper), when actual $\tau = \tau_{SS}$. However, there is a 50% probability of $\hat{\tau}$ being either above or below the mean, actual $\tau$. In this worst case, $P_{HMI}$ is 50%. To ensure there is an acceptable probability, even at this worst case ($\tau = \tau_{SS}$), the threshold is adjusted by adding a multiple of the $\tau$ standard deviation, $k_\tau \sigma_\tau$, to $\tau_{SS}$. The integrity coefficient, $k_\tau$, is determined to ensure a predefined level of integrity. In the right curve of Figure 4, the hazard is now not sensed if the estimated time to closest approach, $\hat{\tau}$, is greater than $\tau_{SS} + k_\tau \sigma_\tau$. In this case, the self-separation integrity risk is the probability of HMI, $P_{HMI}$:

$$P_{HMI} = P(\hat{\tau} > \tau_{SS} + k_\tau \sigma_\tau | \tau \leq \tau_{SS}) \tag{32}$$

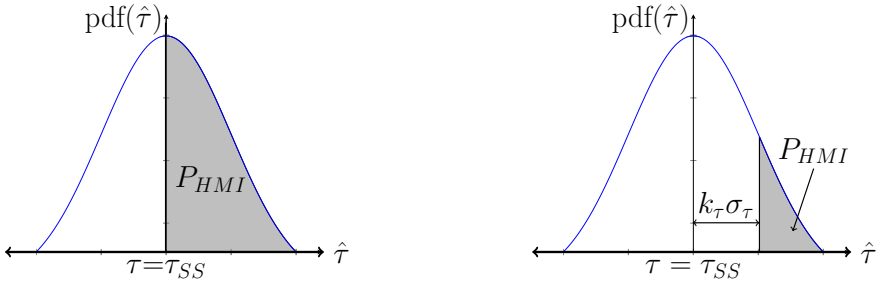


**Figure 4. Integrity Risk when $\tau = \tau_{SS}$ and After Threshold is Adjusted by $k_\tau \sigma_\tau$**

$P_{HMI}$ must meet a predefined integrity risk requirement, $I_\tau$, that will be specified by the FAA's desired level of safety. For the shaded area in the right curve of Figure 4 to be $P_{HMI}$, the integrity risk criterion is expressed as:

$$P_{HMI} = Q(k_\tau) = I_\tau \tag{33}$$

where $Q(x)$ is the tail probability of the standard normal distribution with zero mean and unit variance:

$$Q(x) = 1 - \Phi(x) = \frac{1}{2}\left[1 - \text{erf}\left(\frac{x}{\sqrt{2}}\right)\right] \tag{34}$$

and $\Phi(x)$ is the cumulative distribution function (CDF) for the standard normal distribution:

$$\Phi(x) = \frac{1}{2}\left[1 + \text{erf}\left(\frac{x}{\sqrt{2}}\right)\right] \tag{35}$$

This is used to obtain $k_\tau$:

$$k_\tau = Q^{-1}(I_\tau) \tag{36}$$

$\tau_{SS} + k_\tau\sigma_\tau$ is an adjusted threshold, ensuring that integrity is met. However, the trade-off is that the own aircraft may start its evasive maneuver earlier than $\tau_{SS}$.

### IV.B. Integrity Risk for All Hazard States

In the previous subsection, it was assumed that $\mathbf{x}_{CPA}$ will always violate the WCT and only the $\tau$ hazard was considered. Now we determine full self-separation integrity risk based on $\tau$, $r_{CPA}$, and $z_{CPA}$.

As in the $\tau$ only case, to ensure there is an acceptable $P_{HMI}$ at the worst case for $r$ and $z$ ($r_{CPA} = r_{MD}$ and $z_{CPA} = z_{MD}$), the thresholds are adjusted by adding multiples of the standard deviations to the distance thresholds. The adjusted horizontal CPA miss distance threshold is now $r_{MD}+k_r\sigma_r$ and the adjusted vertical CPA miss distance threshold is now $z_{MD} + k_z\sigma_z$. Now, the self-separation integrity risk is $P_{HMI}$:

$$\text{Sense No Hazard} = [\hat{\tau} > \tau_{SS} + k_\tau\sigma_\tau \ \cup \ \hat{r}_{CPA} > r_{MD} + k_r\sigma_r \ \cup \ \hat{z}_{CPA} > z_{MD} + k_z\sigma_z] \tag{37}$$

$$\text{Hazard Exists} = [\tau \leq \tau_{SS} \ \cap \ r_{CPA} \leq r_{MD} \ \cap \ z_{CPA} \leq z_{MD}] \tag{38}$$

$$P_{HMI} = P[\text{Sense No Hazard}|\text{Hazard Exists}] \tag{39}$$

In equation (39), the condition reflects an imminent (at or within $\tau_{SS}$ seconds) intruder aircraft violation of the WCT. **Hazard Exists** describes a condition where three events occur simultaneously:

- The actual time to closest approach, $\tau$, is less than or equal to $\tau_{SS}$.
- The actual horizontal CPA distance, $r_{CPA}$, is at or within $r_{MD}$.
- The actual vertical CPA distance, $z_{CPA}$, is at or within $z_{MD}$.

The own aircraft should initiate a self-separation maneuver. **Sense No Hazard** describes a case where any of the following three events is occurring:

- The estimated time to closest approach, $\hat{\tau}$, is greater than the adjusted threshold $\tau_{SS} + k_\tau\sigma_\tau$.
- The estimated horizontal CPA, $\hat{r}_{CPA}$, is beyond the adjusted threshold $r_{MD} + k_r\sigma_r$.
- The estimated vertical CPA, $\hat{z}_{CPA}$, is beyond the adjusted threshold $z_{MD} + k_z\sigma_z$.

Any one of these misleading estimates can cause HMI that leads the own aircraft to not maneuver when a self-separation maneuver is warranted. Figure 5 depicts a worst case HMI scenario, where the actual $r_{CPA}$ is just within the $r_{MD}$ but the estimate $\hat{r}_{CPA}$ is just beyond the adjusted threshold $r_{MD} + k_r\sigma_r$. The adjusted threshold ensures that this case occurs with a probability less than or equal to $I_r$ (if we allocate $I_r$ as an integrity requirement specifically for $r_{CPA}$).

$P_{HMI}$ must meet a predefined integrity risk requirement, $I_{SS}$, that will be specified by the certification authority's desired level of safety. This integrity risk criterion for full self-separation is expressed as:

$$P_{HMI} \leq I_{SS} \tag{40}$$

The violation of the integrity limit, $I_{SS}$, reflects a higher than acceptable probability that a self-separation maneuver may be required, but the sensor estimate misleads the SAA system into not maneuvering.

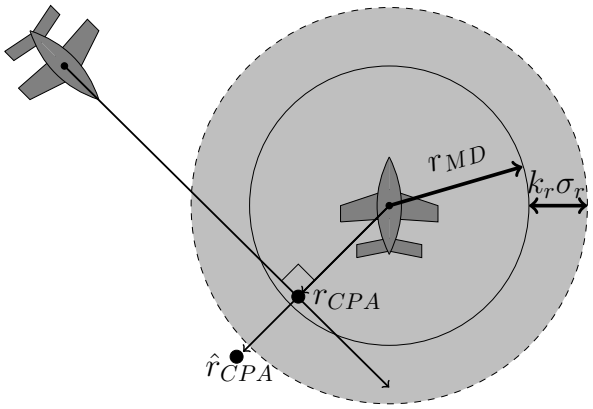


**Figure 5. Worst Case HMI Scenario for $r_{CPA}$**



The hazard state estimates $\hat{\tau}$, $\hat{r}_{CPA}$, and $\hat{z}_{CPA}$ are correlated. In 3D space, the error covariance matrix can be visualized as a tri-variate normal distribution ellipsoid. To illustrate this idea, Figure 6 shows constant probability density ellipses in the 2D $\hat{\tau} - \hat{r}_{CPA}$ plane. The $P_{HMI}$ is the zero-mean joint CDF for this distribution bounded by $[k_\tau\sigma_\tau, \infty]$ in the $\hat{\tau}$ direction and $[k_r\sigma_r, \infty]$ in the $\hat{r}_{CPA}$ direction. In 2D:

$$P_{HMI} \quad = \frac{1}{2\pi|\mathbf{P}_{\mathbf{r}\tau}|^{1/2}} \int_{k_r\sigma_r}^{\infty}\int_{k_\tau\sigma_\tau}^{\infty} e^{(-\frac{1}{2}[\ \tau' \quad r'\ ]^T \mathbf{P}_{\mathbf{r}\tau}{}^{-1}[\ \tau' \quad r'\ ])} d\tau' dr' \tag{41}$$

where $\mathbf{P}_{\boldsymbol{\tau}\mathbf{r}}$ is the upper left 2x2 block of the $\mathbf{P}_{\tau rz}$ matrix and $\tau'$ and $r'$ are integration variables. This is the bivariate normal distribution of $(\hat{\tau}, \hat{r}_{CPA})$, at the worst-case mean vector value of $(\tau_{SS}, r_{MD})$. This is worst-case because of the conditions in equation (41). This double-integral can be evaluated using computation-expensive numerical methods.[14] Ground vehicles can carry the payload necessary to do heavy computations quickly. Aircraft, especially UAS, usually do not. Therefore, the application of DeCleene's and Rife's methods of overbounding on $P_{HMI}$ using univariate normal distributions is more appropriate.[11,12]

In Figure 6, the probability of being in the shaded areas is the integrity risk, $P_{HMI}$. The shaded area to the right of the line $\tau = \tau_{SS} + k_\tau\sigma_\tau$ is accounted for by the Q-function, $Q(k_\tau)$. Likewise, the shaded area above the line $r_{CPA} = r_{MD} + k_r\sigma_r$ is represented by the Q-function, $Q(k_r)$. The probability of the overlap between these two shaded areas is too difficult to evaluate and cannot be evaluated using Q-functions. Instead, we can use an easy-to-compute bound on $P_{HMI}$, which is expressed as:

$$P_{HMI} \leq Q(k_\tau) + Q(k_r) \tag{42}$$

The bound in equation (42) accounts for the probability of being in the overlapping upper-right, shaded quadrant twice, which is conservative, hence the inequality.

Extending this bounding to the full 3D case and applying the integrity risk requirement, $I_{SS}$, the probability of HMI is bounded by the following:

$$P_{HMI} \leq Q(k_\tau) + Q(k_r) + Q(k_z) \leq I_{SS} \tag{43}$$

This bound includes all overlaps between $Q(k_\tau)$, $Q(k_r)$ and $Q(k_z)$, resulting in the inequality. The integrity risk requirement, $I_{SS}$, will be used to allocate the integrity coefficients ($k_\tau$, $k_r$, $k_z$). This could be done, for example, by evenly allocating $I_{SS}$ to the three hazard states. This arbitrary allocation will be readdressed in section VII.

## V. Continuity Risk

This section further quantifies SAA sensor safety by determining continuity risk based on the three hazard states. As we did for integrity, we first assume the CPA distance will be less than the WCT horizontal and vertical miss distances and base continuity risk solely on $\tau$. Then we remove that assumption and base continuity risk on all three hazard states.

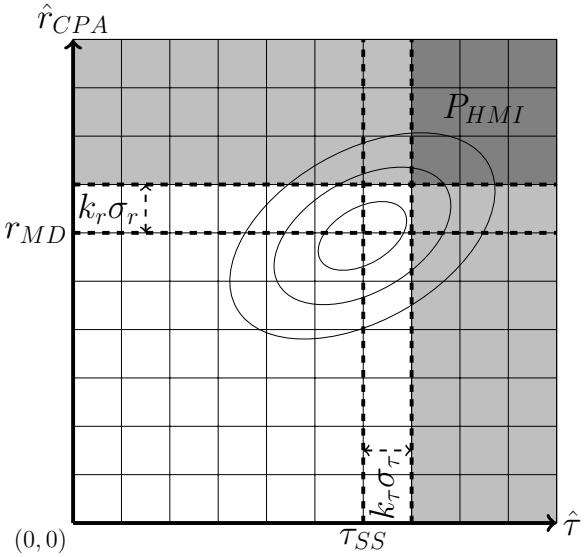


**Figure 6. 2D Integrity Risk Correlation Between Estimated Tau and Estimated Horizontal CPA**



### V.A. Continuity Based Solely on Tau

A false alert occurs when no hazard exists, but a hazard is falsely sensed. Accounting for $\tau$ only, no hazard exists when $\tau > \tau_{SS}$. Accounting for integrity, a hazard is sensed if $\hat{\tau} \leq \tau_{SS} + k_\tau\sigma_\tau$. This FA leads the own aircraft to maneuver when a self-separation maneuver is not warranted.

The left curve in Figure 7 depicts the normal distribution of the estimate, $\hat{\tau}$, when actual $\tau$ is just above the adjusted threshold $\tau_{SS} + k_\tau\sigma_\tau$, where $\mu$ is positive and very small. This accounts for $\hat{\tau} = \tau_{SS} + k_\tau\sigma_\tau$ now being a sensed hazard. In this worst case, there is a 50% probability of $\hat{\tau}$ being either above or below the mean, $\tau_{SS} + k_\tau\sigma_\tau + \mu$. To ensure there is an acceptable FA probability, even at this worst case, a continuity buffer is introduced by adding a multiple of the $\tau$ standard deviation, $\ell_\tau\sigma_\tau$, to the adjusted threshold, $\tau_{SS} + k_\tau\sigma_\tau$. The continuity coefficient, $\ell_\tau$, is determined to ensure a predefined continuity risk requirement, $C_\tau$, that will be specified by the certification authority's desired level of safety. In the right curve of Figure 7, the continuity buffer, $\ell_\tau\sigma_\tau$ is added to the adjusted threshold. In this case, if actual $\tau$ is at or greater than $\tau_{SS} + (k_\tau + \ell_\tau)\sigma_\tau$, then the self-separation continuity risk, $P_{FA}$, is assured to meet $C_\tau$. $P_{FA}$ is defined as:

$$P_{FA} = P(\hat{\tau} \leq \tau_{SS} + k_\tau\sigma_\tau | \tau > \tau_{SS}) \tag{44}$$

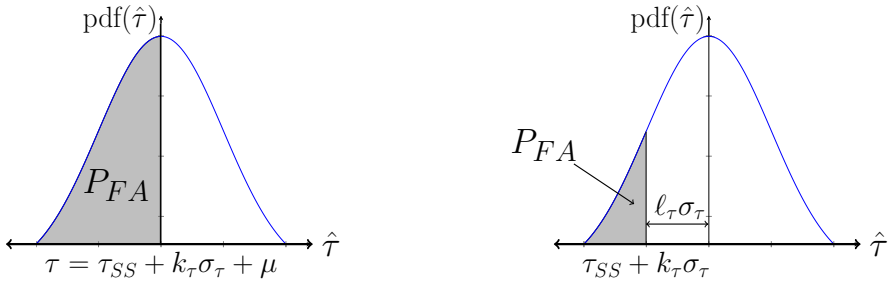


**Figure 7. Continuity Risk when $\tau = \tau_{SS} + k_\tau\sigma_\tau + \mu$ and After Threshold is Further Adjusted by $\ell_\tau\sigma_\tau$**

For the shaded area in the right curve of Figure 7 to be $P_{FA}$, the continuity risk criterion is expressed as:

$$P_{FA} = \Phi(\ell_\tau) = C_\tau \tag{45}$$

where $\ell_\tau$ is a function of $C_\tau$:

$$\ell_\tau = \Phi^{-1}(C_\tau) \tag{46}$$

When $\tau$ is between $\tau_{SS} + k_\tau\sigma_\tau$ and $\tau_{SS} + (k_\tau + \ell_\tau)\sigma_\tau$, the own aircraft may FA with a probability higher than the continuity requirement. This means that the lower limit on protectable $\tau$ is $\tau_{SS} + (k_\tau + \ell_\tau)\sigma_\tau$. We will henceforth call this the $\tau$ *protection level*.

### V.B. Continuity Risk for All Hazard States

As in the $\tau$ only case, to ensure there is an acceptable $P_{FA}$ at the worst case for $r$ and $z$ ($r_{CPA} = r_{MD} + k_r\sigma_r + \mu$ and $z_{CPA} = z_{MD} + k_z\sigma_z + \mu$), continuity buffers are added to the integrity-adjusted distance thresholds. The alert to maneuver will still be based on the integrity-adjusted distance thresholds. The area inside each continuity buffer is where false alerts can occur with a probability higher than a given continuity requirement. The self-separation continuity risk is $P_{FA}$:

$$\text{Sense Hazard} = [\hat{\tau} \leq \tau_{SS} + k_\tau\sigma_\tau \ \cap \ \hat{r}_{CPA} \leq r_{MD} + k_r\sigma_r \ \cap \ \hat{z}_{CPA} \leq z_{MD} + k_z\sigma_z] \tag{47}$$

$$\text{No Hazard Exists} = [\tau > \tau_{SS} \ \cup \ r_{CPA} > r_{MD} \ \cup \ z_{CPA} > z_{MD}] \tag{48}$$

$$P_{FA} = P(\text{Sense Hazard}|\text{No Hazard Exists}) \tag{49}$$

Figure 8 depicts a worst case FA scenario, where the actual $r_{CPA}$ is just beyond the protection level $r_{MD} + k_r\sigma_r + \ell_r\sigma_r$ while the estimate $\hat{r}_{CPA}$ is just within the integrity-adjusted threshold $r_{MD} + k_r\sigma_r$. The continuity buffer ensures this case occurs with a probability less than or equal to $C_r$ (if we allocate $C_r$ as a continuity requirement specifically for $r_{CPA}$).

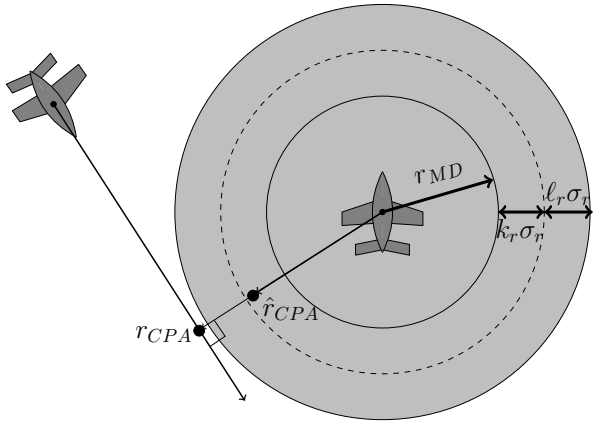


**Figure 8. Worst Case FA Scenario for $r_{CPA}$**

$P_{FA}$ must meet an overall predefined continuity requirement, $C_{SS}$, that will be specified by the certification authority's desired level of safety. The continuity risk criterion is expressed as:

$$P_{FA} \leq C_{SS} \tag{50}$$

To illustrate, Figure 9 shows the constant probability density ellipses in the 2D $\hat{\tau} - \hat{r}_{CPA}$ plane. We will apply the same overbounding methods as the integrity risk of the previous section. In Figure 9, $P_{FA}$ is the dark shaded area of the lower left corner. The probability of being in the shaded areas to the left of the line $\hat{\tau} = \tau_{SS} + k_\tau\sigma_\tau$ is given by the $\Phi$ function, $\Phi(\ell_\tau)$. Likewise, the probability of being in the shaded areas below line $\hat{r}_{CPA} = r_{MD} + k_r\sigma_r$ is given by the $\Phi$ function, $\Phi(\ell_r)$. The probability of the overlap between these two shaded areas is difficult to evaluate and cannot be evaluated using $\Phi$ functions. Instead, we can use an easy-to-compute bound on $P_{FA}$, which is expressed as:

$$P_{FA} \leq \frac{\Phi(\ell_\tau) + \Phi(\ell_r)}{2} \tag{51}$$

The conservative bound in equation (51) accounts for the probability of being in the overlapping lower-left, shaded quadrant and the excess probabilities in the lighter shaded areas.

Extending this bounding to the full 3D case and applying the continuity risk requirement, $C_{SS}$, the probability of FA is bounded by the following:

$$P_{FA} \leq \frac{\Phi(\ell_\tau) + \Phi(\ell_r) + \Phi(\ell_z)}{3} \leq C_{SS} \tag{52}$$

This bound accounts for the overlaps and excesses between $\Phi(\ell_\tau)$, $\Phi(\ell_r)$, and $\Phi(\ell_z)$. The continuity risk requirement, $C_{SS}$, will be used to allocate the continuity coefficients ($\ell_\tau$, $\ell_r$, $\ell_z$). As in the integrity case, this could be done, for example, by evenly allocating $C_{SS}$ to the three hazard states. This arbitrary allocation will be readdressed in section VII.

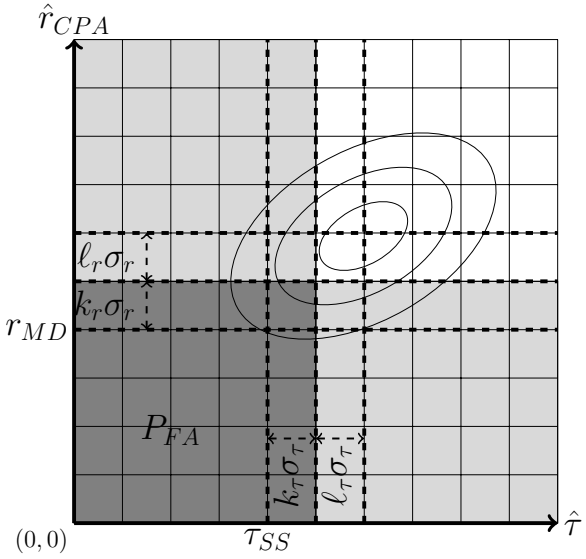


**Figure 9. 2D Continuity Risk Correlation Between Estimated Tau and Estimated Horizontal CPA**

## VI. Relating Integrity and Continuity to Sensor Requirements

With a predefined integrity risk requirement, $I_{SS}$, and a predefined continuity requirement, $C_{SS}$, the SAA system will alert and maneuver depending on how large each hazard state standard deviation ($\sigma_\tau$, $\sigma_r$, and $\sigma_z$) is at each sampled time. All hazard state $\sigma$ values are functions of the sensor uncertainty, the sensor range, and the sample interval, $\Delta t$. The number of samples, $n$, will depend on sensor range, $\Delta t$, and the relative intruder velocity, $\dot{\mathbf{x}}$. As the SAA system gets more intruder measurements, each hazard state standard deviation will get smaller over time.

### VI.A. Operational Limits

Each hazard state's protection level must be reasonably close to the original WCT before a hazard test can be executed. If the protection level is too big, the resulting protected separation distances can be very large, leading to ATC capacity issues. To mitigate this, a certification authority will need to determine an acceptable percentage, $\epsilon$, of all three original hazard thresholds ($\tau_{SS}$, $r_{MD}$, and $z_{MD}$) for $(k+\ell)\sigma$. This is defined as:

$$\epsilon = \frac{(k_\tau + \ell_\tau)\sigma_\tau}{\tau_{SS}} = \frac{(k_r + \ell_r)\sigma_r}{r_{MD}} = \frac{(k_z + \ell_z)\sigma_z}{z_{MD}} \tag{53}$$

This $\epsilon$ can define constant operational limits on hazard state standard deviations, $\tilde{\sigma}$, and on hazard states themselves ($\tilde{\tau}_\tau$, $\tilde{r}_{CPA}$, $\tilde{z}_{CPA}$). The hazard state standard deviation operational limits are:

$$\begin{aligned} \tilde{\sigma}_\tau &\triangleq \tfrac{\epsilon\tau_{SS}}{k_\tau+\ell_\tau} \\ \tilde{\sigma}_r &\triangleq \tfrac{\epsilon r_{MD}}{k_r+\ell_r} \\ \tilde{\sigma}_z &\triangleq \tfrac{\epsilon z_{MD}}{k_z+\ell_z} \end{aligned} \tag{54}$$

The hazard state operational limits are:

$$\begin{aligned} \tilde{\tau}_\tau &\triangleq (1+\epsilon)\tau_{SS} \\ \tilde{r} &\triangleq (1+\epsilon)r_{MD} \\ \tilde{z} &\triangleq (1+\epsilon)z_{MD} \end{aligned} \tag{55}$$

The CPA distance hazard state operational limits ($\tilde{r}$ and $\tilde{z}$) can be translated to operational limits on $\tau$ because there is an associated time to CPA when these limits are reached. The $\tau$'s when $r$ and $z$ cross their respective operational limits ($\tilde{r}$, $\tilde{z}$) can be determined based on the constant velocity model. Figure 10 depicts an example of this for the intruder horizontal range, $r$. When the intruder horizontal range, $r$, crosses the horizontal range operational limit, $\tilde{r}$, the $\tau$ associated with $r = \tilde{r}$ is $\tilde{\tau}_r$. This will be compared with $\tilde{\tau}_\tau$ and $\tilde{\tau}_z$ to determine the appropriate $\tilde{\tau}$ to apply to the $\sigma_r$ vs $\tau$ curve for analysis.

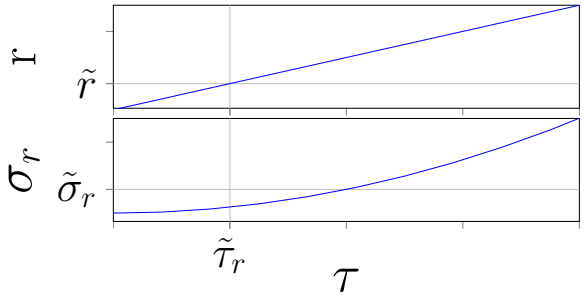


**Figure 10. Hazard State $\tilde{\tau}_r$ for Horizontal CPA Distance**

Typically, because $\tilde{\tau}_r$ and $\tilde{\tau}_z$ will be very small and much lower than $\tilde{\tau}_\tau$, the operational limit on $\tau$, $\tilde{\tau}$, will usually be determined by $\tilde{\tau}_\tau$ for all three hazard states and labeled as $\tilde{\tau}$. However, if $\epsilon$ is selected to be very large, $\tilde{\tau}_r$ and $\tilde{\tau}_z$ may need to be considered. $\tilde{\tau}$ is the maximum of each of the three hazard state $\tilde{\tau}$'s:

$$\tilde{\tau} = \max(\tilde{\tau}_\tau, \tilde{\tau}_r, \tilde{\tau}_z) \tag{56}$$

## VI.B. Relating $\sigma_\tau$ to Sensor Requirements

Figure 11 depicts how the operational limit relates to sensor requirements. Each plot is a hazard state $\sigma$ versus $\tau$. Within the three plots are three curves representing three different sensors. For a sensor to meet requirements, each $\sigma$ curve must cross its $\tilde{\sigma}$ at a $\tau$ greater than $\tilde{\tau}$. If a sensor $\sigma$ curve crosses its $\tilde{\sigma}$ at a $\tau$ less than $\tilde{\tau}$, it will cross into the gray shaded area, which indicates a sensor that will FA at a probability higher than the continuity risk requirement. In the figure, only the bottom sensor, Sensor 3, meets the continuity risk requirement.

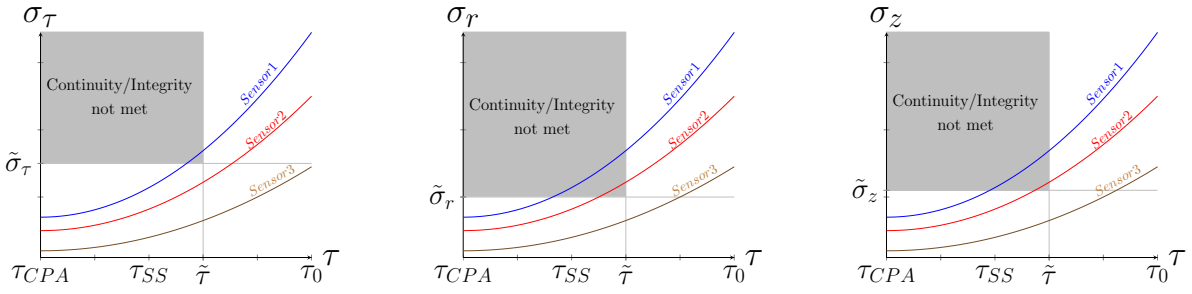


**Figure 11. Applying Operational Limits to Sensor Requirements**

## VI.C. Applying Self-Separation Tests

In order to apply this methodology, a sensor must have characteristics (sensor uncertainty, sensor range, and sample interval) to reduce each hazard state $\sigma$-value below each $\tilde{\sigma}$ prior to its $\tilde{\tau}$, as depicted in Figure 11.

If a given sensor is not good enough, sensor uncertainty must be improved, sensor range must be extended, and/or sample intervals must be reduced.

In order to maintain continuity, a minimum number of self-separation tests must be accomplished. For a constant velocity model, once all three hazard state $\sigma$'s are reduced below their $\tilde{\sigma}$, there only needs to be one test. From there, an alerted UAS can maneuver based on timing: when $\hat{\tau} < \tilde{\tau}$.

## VII. Sensitivity Analysis

This sensitivity analysis assumes a two-dimensional scenario and addresses how the improvement of sensor parameters relate to meeting integrity and continuity requirements. We start with the nominal spherical sensor described in the Edwards paper,[15] where $\sigma_\rho$ is 24.6 feet, $\sigma_\theta$ is 0.24 degrees, and range is 8 nautical miles (NM). The spherical sensor uncertainty and error covariance are transformed into Cartesian coordinates using a first-order Taylor Series transformation. For simplicity, we use a sample interval, $\Delta t$, of 1 second. A worst-case relative velocity of 500 knots is chosen, reflecting the closure of two aircraft at a maximum airspeed of 250 knots each. Aircraft are restricted to 250 knots below 10,000 feet per 14 CFR 91.117.[16] The WCT established by RTCA SC-228 is used: $\tau_{SS}$ of 35 seconds and an $r_{MD}$ of 4000 feet.[7] The intruder aircraft trajectories were varied from head-on to a tangent trajectory to the $r_{MD}$ circle. An $\epsilon$ of 10% is chosen leading to $\tilde{\tau}_\tau$ of 38.5 seconds and $\tilde{r}_{MD}$ of 4400 feet. The desired integrity requirement, $I_{SS} = 10^{-6}$, and the continuity requirement, $C_{SS} = 10^{-5}$, are based on the FAA's definition of major hazards.[9] For simplicity, $k_\tau$ and $k_r$ are set to be equal, resulting in $k_\tau = k_r = 4.89$. Similarly, $\ell_\tau = \ell_r = 4.26$. The corresponding operational limits are a $\tilde{\sigma}_\tau$ of 0.38 seconds and a $\tilde{\sigma}_r$ of 43.68 feet.

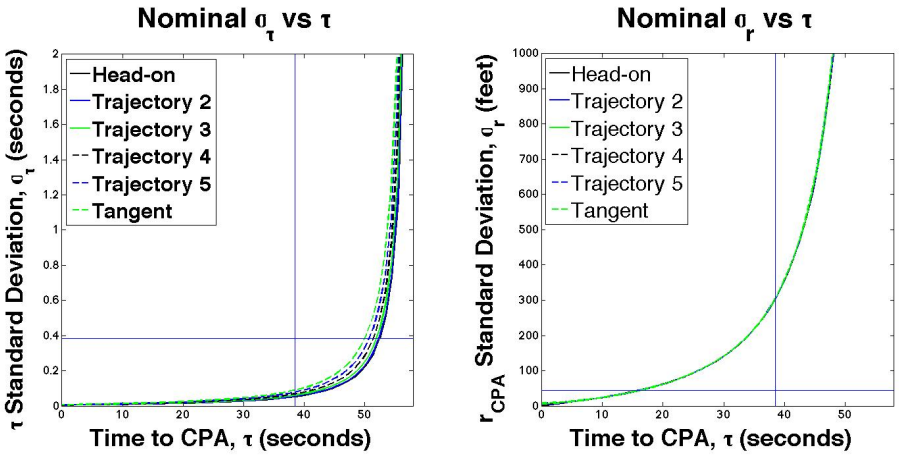


**Figure 12. Results of a Nominal Sensor**

The results from the nominal case are in Figure 12. Here, all trajectories meet $\sigma_\tau$ requirements, but none meet $\sigma_r$. In the $\sigma_\tau$ curve, the tangent trajectory most restrictive. The trajectories are indistinguishable for the $\sigma_r$ curve.

The first adjustment of the sensitivity analysis improves sensor $\theta$ uncertainty by a factor of 10. $\sigma_\theta$ is now 0.024 degrees. The results in Figure 13 depict this $\theta$-adjusted sensor now meeting both $\sigma_\tau$ and $\sigma_r$ requirements for all trajectories.

The next adjustment improves sensor $\rho$ uncertainty by a factor of 10. $\sigma_\rho$ is now 2.46 feet. Sensor $\theta$ uncertainty is returned to 0.24 degrees. The results in Figure 14 depict this $\rho$-adjusted sensor meeting $\sigma_\tau$ requirements, but not meeting $\sigma_r$ requirements (for all trajectories). It is worth noting the most restrictive trajectory (corresponding to the curve above all others) for $\sigma_r$ is the head-on trajectory, in contrast with $\sigma_\tau$, where it is the tangential trajectory.

We repeat this process twice by first doubling sensor range from 8NM to 16NM and then by reducing the sample interval from 1 second to 0.1 seconds. The results of the nominal and all four parameter adjustments are compiled in Figure 15, where the most restrictive trajectories (tangential) are applied to the $\sigma_\tau$ curve and the most restrictive trajectories (head-on) are applied to the $\sigma_r$ curve. For the $\sigma_r$ curve, the $\sigma_\theta$ adjustment is the only one meeting requirements. The next best parameter is range, followed by $\Delta t$ and, lastly, $\sigma_\rho$,

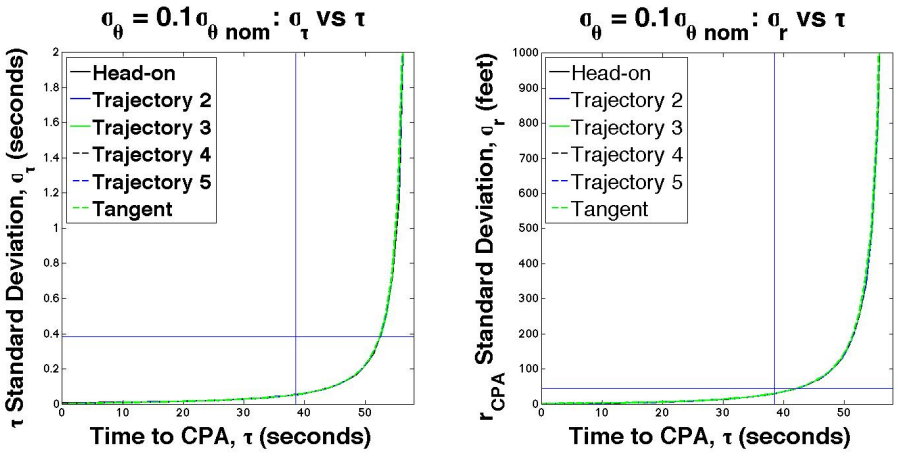


**Figure 13. Results of a $\theta$-Adjusted Sensor: $\sigma_\theta = 0.024$ degrees**

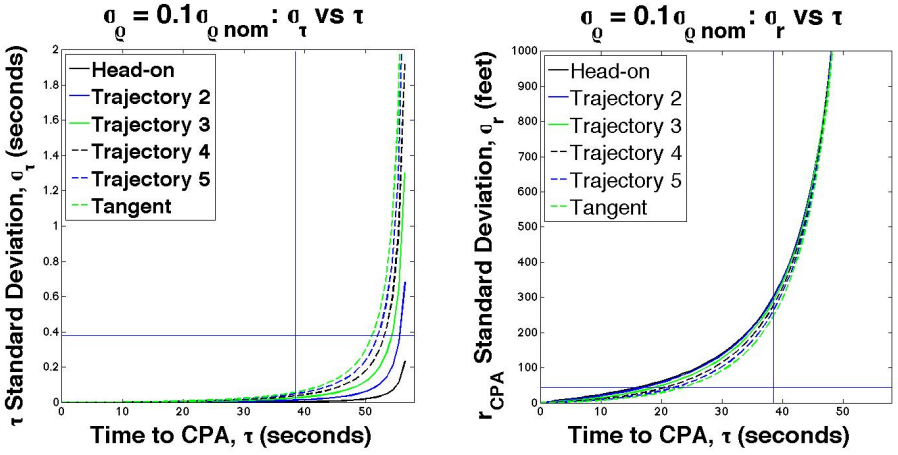


**Figure 14. Results of a $\rho$-Adjusted Sensor: $\sigma_\rho = 2.46$ feet**

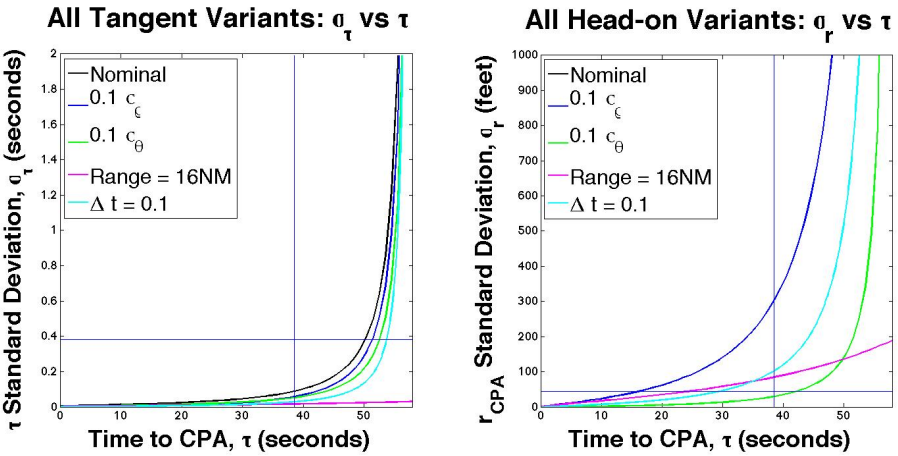


**Figure 15. Results of All Sensor Parameter Adjustments**

which does not show any improvement over the nominal curve. For $\sigma_\tau$, all curves meet requirements, where the range adjustment provides the most margin in clearing the requirement, then $\Delta t$, followed by $\sigma_\theta$ and, finally, $\sigma_\rho$.

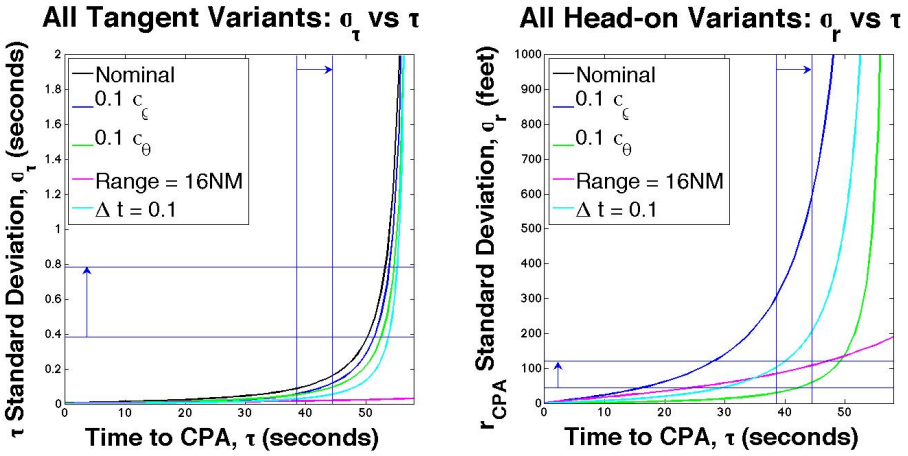


**Figure 16. All Sensor Parameter Adjustments with Improved $\tilde{\sigma}$'s**

Another sensitive parameter is the allocation of integrity and continuity between hazard states. The nominal allocation is arbitrarily even across hazard states. However, in this example, $r$ is more restrictive than $\tau$. The intention is to maximize the risk allocation on $r$, by reducing $k_r$ and $\ell_r$ to increase $\tilde{\sigma}_r$. The trade-off is, following equations (43) and (52), a corresponding increase of $k_\tau$ and $\ell_\tau$ and decrease of $\tilde{\sigma}_\tau$ in equation (54). Following equations (43) and (52) again, there is a limit to how much risk you can place on $r$ based on $I_{SS}$ and $C_{SS}$. In this case, the minimum $k_r$ of 4.7535 and $\ell_r$ of 4.1075 leads to a maximum $\tilde{\sigma}_r$ of 45 feet, which in this example, does not provide significant improvement as compared to the nominal case.

Another option to meet integrity and continuity, if acceptable to the certification authority, is increasing $\epsilon$, which relaxes the operational limits ($\tilde{\tau}$'s and $\tilde{\sigma}$'s). In this case, we increase $\epsilon$ to increase $\tilde{\sigma}_r$. For example, if we want a $\tilde{\sigma}_r$ of 120 feet to have the range-adjusted sensor meet requirements, $\epsilon$ must increase to 0.27. The impact on $\tau$ is $\tilde{\sigma}_\tau$ increases to 0.78 seconds and $\tilde{\tau}$ increases to approximately 44 seconds. This leads to the range-adjusted sensor meeting all requirements, as reflected in Figure 16. The problem with increasing $\epsilon$ is that it increases the protection levels. This, in turn, reduces airspace capacity. For example, the integrity and continuity adjusted horizontal miss distance increases from 4400 feet to 5063 feet.

In conclusion, reducing the nominal sensor $\sigma_\theta$ and increasing its range have the most impact on the UAS SAA integrity and continuity performance. Reallocation of integrity and continuity risk requirements can also help improve performance. Finally, if the certification authority allows modification of the operational limit parameter $\epsilon$, then sensor requirements are relaxed, but airspace capacity is reduced.

## VIII. Conclusions

There is currently high interest in providing greater UAS access into the NAS. The FAA will require UAS to employ SAA systems to make this a reality. To ensure an acceptable level of safety, UAS SAA systems must sense intruders to initiate avoidance maneuvers. Integrity and continuity risk requirements can ensure this level of safety and lead to meaningful, certifiable SAA sensor requirements.

In this paper, a methodology was presented for determining integrity and continuity risk based on a constant, relative velocity model with normal, independent and stationary measurement errors. Adjusted thresholds and continuity buffers were derived to account for integrity and continuity risk caused by sensor uncertainty. A sensitivity analysis, assuming a two dimensional co-altitude intruder with horizontal only trajectory, was presented showing how adjusting sensor parameters could meet safety requirements. Ultimately, this research can help determine SAA requirements on specific sensors based on high-level integrity and continuity requirements.

Opportunities for future work include extending the analysis to three dimensional intruder trajectories, addressing the case of multiple intruders, accounting for accelerations and testing on hardware.

## Acknowledgments

We would like to express our appreciation to John Warburton, Navigation Branch Manager, and Phil Maloney, UAS Certification Obstacle Team Leader, both of the FAA Hughes Technical Center, for supporting this research, which was recently awarded FAA Grant #14-G-018. However, the views expressed in this paper are the authors' alone and do not necessarily represent the opinions of any other organization or person.

## References

[1]Federal Aviation Administration, "Integration of Civil Unmanned Aircraft Systems (UAS) in the National Airspace System (NAS) Roadmap," Nov 2013.

[2]US House of Representatives, "FAA Modernization and Reform Act of 2012," Feb 2012.

[3]Federal Aviation Administration TCAS Program Office, "Concept of Use for the Airborne Collision Avoidance System $X_U$," Feb 2013.

[4]Federal Aviation Administration, "Sense and Avoid (SAA) for Unmanned Aircraft Systems (UAS), SAA Workshop Second Caucus Report," Jan 2013.

[5]14 CFR 91.113, "Right-of-way Rules: Except Water Operations," Jul 2004.

[6]Weibel, R. E., Edwards, M. W. M., and Fernandes, C. S., "Establishing a Risk-Based Separation Standard for Unmanned Aircraft Self Separation," *Ninth USA/Europe Air Traffic Management Research and Development Seminar*, Berlin, Germany, Jun 2011.

[7]Davis, D. A., "RTCA Standards Committee Grapples with UAS Collision Avoidance Rules," *Inside GNSS News*, Aug 2014.

[8]Pullen, S., "What are the Differences Between Accuracy, Integrity, Continuity, and Availability, and How are they Computed?" *InsideGNSS*, Sep-Oct 2008, pp. 20–24.

[9]Federal Aviation Administration, "Advisory Circular 25.1309-1A - System Design and Analysis," Jun 1988.

[10]RTCA SC-159, "Minimum Aviation System Performance Standards for the Local Area Augmentation System," 2004.

[11]DeCleene, B., "Defining Pseudorange Integrity - Overbounding," *Institute of Navigation GPS Conference*, Salt Lake City, UT, Sep 2010, pp. 1916–1924.

[12]Rife, J., Pullen, S., Enge, P., and Pervan, B., "Paired Overbounding for Non-ideal LAAS and WAAS Error Distributions," *IEEE Transactions on Aerospace and Electronic Systems*, Vol. 42, No. 4, Oct 2006, pp. 1386–1395.

[13]RTCA SC-147, "Minimum Operational Performance Standards for Traffic Alert and Collision Avoidance System II," 2008.

[14]Drezner, Z., "Computation of the Trivariate Normal Integral," *Mathematics of Computation*, Vol. 63, 1994, pp. 289–294.

[15]Edwards, M., "A Safety Driven Approach to the Development of an Airborne Sense and Avoid System," *AIAA Infotech@Aerospace*, Garden Grove, CA, Jun 2012.

[16]14 CFR 91.117, "Aircraft Speed," Aug 1993.